ELSEVIER

International Journal of Mass Spectrometry 213 (2002) 237–250

International Journal of Mass Spectrometry

www.elsevier.com/locate/ijms

The gas-phase sodium basicities of common matrix-assisted laser desorption/ionization matrices

Juan Zhang, Richard Knochenmuss, Elizabeth Stevenson, Renato Zenobi*

[a]*Laboratory of Organic Chemistry, Swiss Federal Institute of Technology (ETH) ETH-Hönggerberg HCI, CH-8093 Zürich, Switzerland*

Received 9 April 2001; accepted 9 October 2001

Abstract

The gas-phase sodium basicities (GNaB) of common matrix-assisted laser desorption/ionization (MALDI) matrices were determined in a Fourier transform ion cyclotron resonance mass spectrometer (FT ICR MS) by monitoring the sodium ion transfer reaction between sodiated matrix molecules and a reference base with known gas-phase sodium basicity. The data was analyzed by two methods: one where the equilibrium constant was determined directly from ion concentrations at equilibrium and the other based on fitting the reaction kinetics over the full reaction time scale. Fitting of the reaction kinetics solved the problem of competing reactions, i.e. formation of sodium bound dimers, which complicates direct determination of the equilibrium constant. The gas-phase sodium ion basicities of twelve MALDI matrices were found to lie between 140–170 kJ mol^{-1}. The activation energy of the rate-limiting step was also determined. (Int J Mass Spectrom 213 (2002) 237–250) © 2002 Elsevier Science B.V.

Keywords: Gas-phase; GNaB; MALDI

1. Introduction

Cationization, together with protonation/deprotonation and electron transfer, is a major secondary ionization processes in matrix-assisted laser desorption/ionization (MALDI) [1,2]. Much work is currently being done to study MALDI ionization mechanisms [3–5], including investigation of proton transfer and gas-phase proton affinities/basicities of MALDI matrices [6–10], study of matrix suppression effects [11,12], and cationization processes [13–18]. Synthetic polymers are often observed in MALDI mass spectra in cationized form [14,15,19–23]. For this reason, metal salts are often added into MALDI samples for polymer analysis, in order to enhance the signal. Cationized proteins, peptides, and biopolymers have also been observed in MALDI mass spectra [24–26].

On the other hand, cationization can also deteriorate the quality of MALDI spectra. For example, multiple metal ion adducts in the MALDI mass spectra of oligosaccharides can complicate the interpretation of the data and prevent rapid identification of the components in a complex mixture [27]. Cationization, which is generally thought to occur in the gas-phase [19,20], must obviously be controlled, so that its advantages can be exploited and its disadvantages alleviated. For this reason, thermodynamic and kinetic data are necessary for understanding cation-

* Corresponding author. E-mail: zenobi@org.chem.ethz.ch

PII S1387-3806(01)00542-5

ization reactions in the MALDI plume. Ion formation in MALDI, including cationization, has been proposed to be largely under thermodynamic control [2]. Fundamental data on MALDI matrices, such as gas-phase proton affinities and basicities, are therefore appearing in the literature more and more frequently [8,9,28–30]. In contrast to proton transfer, the thermodynamics of metal ion transfer has not been investigated in similar detail. This is the aim of the present paper.

Sodium is by far the most important ion forming cationized signals in MALDI mass spectrometry (MS). Na^+ is ubiquitous, and sodiated molecules are almost always observed in MALDI mass spectra, even without adding salt to the samples. In the mass spectra of pure 2,5-dihydroxy benzoic acid (DHB), for example, the sodiated molecular ion signal shows up with significant relative intensity next to the $(M+H)^+$ signal, due to only trace amounts of sodium present in the DHB. The gas-phase sodium affinities/basicities of small molecules such as H_2, N_2, and H_2O, organic, and small biological molecules have been determined experimentally and theoretically in previous work [31–39]. However, values for the gas-phase sodium affinities/basicities of MALDI matrices are largely unknown. The gas-phase sodium ion affinities/basicities of a range of important MALDI matrices are reported here.

Different methods have been employed for determination of the gas-phase sodium ion affinities/basicities of organic and inorganic molecules, including Cook's kinetic method [31,39–42], the threshold collision-induced dissociation (CID) technique, [32,33,43–45], and the equilibrium method using high-pressure mass spectrometry (HPMS) [37,38,46]. Cook's kinetic method is based on monitoring the dissociation rate of the sodium-bound hetro dimer in both directions. The laser desorption employed in our FT ICR renders the formation of the metal ion-bound dimer for some matrices difficult. Although some hetro dimer forms after a certain reaction time and can, in principle, be isolated for kinetic measurements, the signal-to-noise ratio is quite low. Consequently, this method is not suitable for these studies. The threshold CID method requires a fairly involved theoretical treatment of the data, along with specialized equipment. The equilibrium method using HPMS can only be employed for determination of gas-phase metal ion affinity of organic molecules that are rather volatile.

The FT ICR experiments in our group are carried out at room temperature. Laser desorption was used to generate sodiated matrices in the gas-phase. A reference base with known gas-phase sodium basicity and high vapor pressure was chosen such that the sodium-transfer reaction from the sodiated matrix to the reference base can be studied and the course of this reaction followed. In addition to the relative amounts of the ionic reaction partners at equilibrium, the complete kinetics of the sodium ion transfer reaction is also available from the experiment. Therefore, we chose to determine the equilibrium constant by two methods. The first was a direct determination of the equilibrium constant, which is based on observation of reagent and product concentrations at equilibrium. This suffered from competing side reactions. In the second method, the entire reaction kinetics was fit to a model, and the rate constants were adjusted to obtain the best quality fit. In this fashion, the appropriate rate constants could be determined even in the presence of side reactions.

Quantum chemical calculations methods have also been used to study the gas-phase sodium binding energies and affinities [31,33,37,43,47]. In this work, we only report preliminary results for one matrix.

2. Methods

2.1. Direct determination of equilibrium constant

The gas-phase sodium ion basicity (GNaB) is defined as the negative of the free energy for

$$M + Na^+ \xrightarrow{\Delta G_1} [M + Na]^+ \quad (1)$$

$$-\Delta G_1 = \mathrm{GNaB(M)}$$

or

$$Re + Na^+ \xrightarrow{\Delta G_2} [Re + Na]^+ \quad (2)$$

$$-\Delta G_2 = \mathrm{GNaB(Re)}$$

where M is the matrix and Re is a reference base.

In the gas-phase, the sodium transfer reactions take place between a sodiated matrix molecule and a neutral reference base molecule (Re), as shown in

$$[M + Na]^+ + Re \overset{\Delta G}{\rightleftharpoons} M + [Re + Na]^+ \quad (3)$$

The free energy change for this reaction is the difference between the gas-phase sodium basicities of the matrix GNaB(M) and the reference base GNaB(Re).

$$\Delta G = \Delta G_2 - \Delta G_1 = GNaB(Re) - GNaB(M) \quad (4)$$

The relationship between the free energy and reaction equilibrium constant can be written as:

$$GNaB(M) = GNa(Re) - RT \cdot \ln K_{eq} \quad (5)$$

The equilibrium constant K_{eq} for the sodium ion transfer reaction is:

$$K_{eq} = \frac{[Re + Na)^+] \cdot [M]}{[(M + Na)^+] \cdot [Re]} \quad (6)$$

The ratio $[(Re + Na)^+]/[(M + Na)^+]$ can be obtained from the mass spectra, whereas the ratio of the neutrals [M]/[Re] must be determined separately.

2.2. Fit of the reaction kinetics

Gas-phase sodium basicities can be determined by the equilibrium method only in the absence of competing reaction channels. However, in many of the systems studied here, species other than sodiated matrix and sodiated reference base were observed. The sodium ion transfer reaction was generally found to begin with the formation of a small amount of sodium-bound hetro dimer, followed by its dissociation to products, as shown in

$$[M + Na]^+ + Re \underset{k_{-1}}{\overset{k_1}{\rightleftharpoons}} [M + Na + Re]^+ \underset{k_{-2}}{\overset{k_2}{\rightleftharpoons}} M + [Re + Na]^+ \quad (7)$$

Furthermore, a sodiated reference molecule can form an adduct with another neutral reference molecule, and a sodium-bound homo dimer results.

$$[Re + Na]^+ + Re \underset{k_{-3}}{\overset{k_3}{\rightleftharpoons}} [Re + Na + Re]^+ \quad (8)$$

After several seconds reaction time, the sodium bound homo dimer $[Re + Na + Re]^+$ can sometimes be the dominant species (Fig. 1). This reaction also shifts the previous reaction equilibrium to the right side and thus leads to a systematic error in determining the reaction equilibrium constant according to Eq. 6.

In order to take reaction 8 explicitly into account, we fitted the complete kinetic data. For this we considered the following two models:

Model 1.

$$[M + Na]^+ + Re \underset{k_{-1}}{\overset{k_1}{\rightleftharpoons}} [M + Na + Re]^+ \underset{k_{-2}}{\overset{k_2}{\rightleftharpoons}} M + [Re + Na]^+ + (Re) \underset{k_{-3}}{\overset{k_e}{\rightleftharpoons}} [Re + Na + Re]^+ \quad (9)$$

Model 2.

$$[M + Na]^+ + Re \underset{k_{-1}}{\overset{k_1}{\rightleftharpoons}} \begin{matrix} [Re + Na + Re]^+ \\ k_3 \Downarrow \Uparrow k_{-3} \\ + Re \\ [M + Na + Re]^+ \end{matrix} \underset{k_{-2}}{\overset{k_2}{\rightleftharpoons}} M + [Re + Na]^+ \quad (10)$$

Both of these two models include six rate constants (k_1, k_{-1}, k_2, k_{-2}, k_3, k_{-3}), and six species, among

them the four observable ions: $[M + Na]^+$, $[M + Na + Re]^+$, $[Re + Na]^+$, $[Re + Na + Re]^+$. Since the partial pressures of the neutral reference base [Re] and the neutral matrix [M] are constant, we have four differential equations for the time dependent concentrations of each of the four ionic species. The concentration of every ionic species is normalized to the total concentration of ions. The relative concentration of two neutrals in comparison with the total concentration of ions was kept constant in the fits.

To fit the data, i.e. the time dependence of the normalized ion signal intensities, these differential equations were integrated numerically using 4th order Runge-Kutta methods with adaptive step size [48]. The Simplex method was used for fitting [48]. The fits were started considering only a small time range, where the ion signal ratio changes most rapidly, then expanded to the whole reaction time range using the rate constants obtained by the small time range fit as initial guess. This procedure was repeated several times until the best fit was found. The k values obtained from the last fit were used for determining the desired equilibrium constant,

$$K_{eq} = \frac{k_1 \cdot k_2}{k_{-1} \cdot k_{-2}} \tag{11}$$

and hence the GNaB.

2.3. Activation energy G_a

The presence of an energy barrier for sodium ion transfer results in a reduction of the reaction rates below the collision rates. Reasons for this are charge delocalization and steric hindrance [49], which have more of an influence in the case of gas-phase metal ion transfer reactions than for proton transfer reactions, due to higher polarizabilities and larger size of metal ions compared to protons.

The relation between the activation energy G_a and the corresponding rate constant k is presented in [50],

$$G_a = -RT \ln\left(\frac{k}{k_{coll}}\right) \tag{12}$$

where k_{coll} is the collision rate constant for gas-phase reactions. The collision rate constant k_{coll} of ions and neutral molecules can be obtained from "Langevin" model:[51]

$$k_{coll} = \sqrt{\frac{4\pi^2 \cdot \alpha' \cdot q^2}{\mu}} \quad \text{(cgs. units)} \tag{13}$$

where α' is the isotropic polarizability of the neutral, q is the ion charge, and μ is the reduced mass of the collision partners, namely, the sodiated matrix and the neutral reference base. For dimethoxyethane (DME), which was used in this work the reference base, α' is 9.56×10^{24} cm^3 [52]. The rate constant k is obtained from the fitting procedure described above.

3. Experimental section

All experiments were performed on a Fourier transform ion cyclotron resonance mass spectrometer (FT ICR MS) with an elongated cylindrical cell. The instrument is equipped with a 4.7 tesla superconducting magnet (Bruker, Fällanden, Switzerland) and Odyssey data acquisition electronics (Finnigan, Madison, WI). A Nd:YAG laser (Minilite ML-10, Continuum, CA) operated at 355 nm was employed for laser desorption. The typical laser irradiance was 4×10^6 W cm^{-2}.

Sodiated matrix molecules were generated by laser desorption of the sample made with a mixture of matrix and sodium chloride dissolved in water or a water/ethanol solution. 20 μl of this solution were dropped on a target and allowed to dry at room temperature. This drop-and-dry procedure was repeated several times until there was a good crystal layer covering the surface of target. Some matrices, e.g. 6-aza-2-thiothymine, nicotinic acid do not absorb the laser irradiation at 355 nm very well, desorption was improved with the two-phase method [53]. In these cases, the matrix/NaCl solution was mixed with an equal volume of silicon particles. This mixture was dropped on the target and allowed to dry.

An internal ion source was employed on our instrument. The solid sample was placed right behind

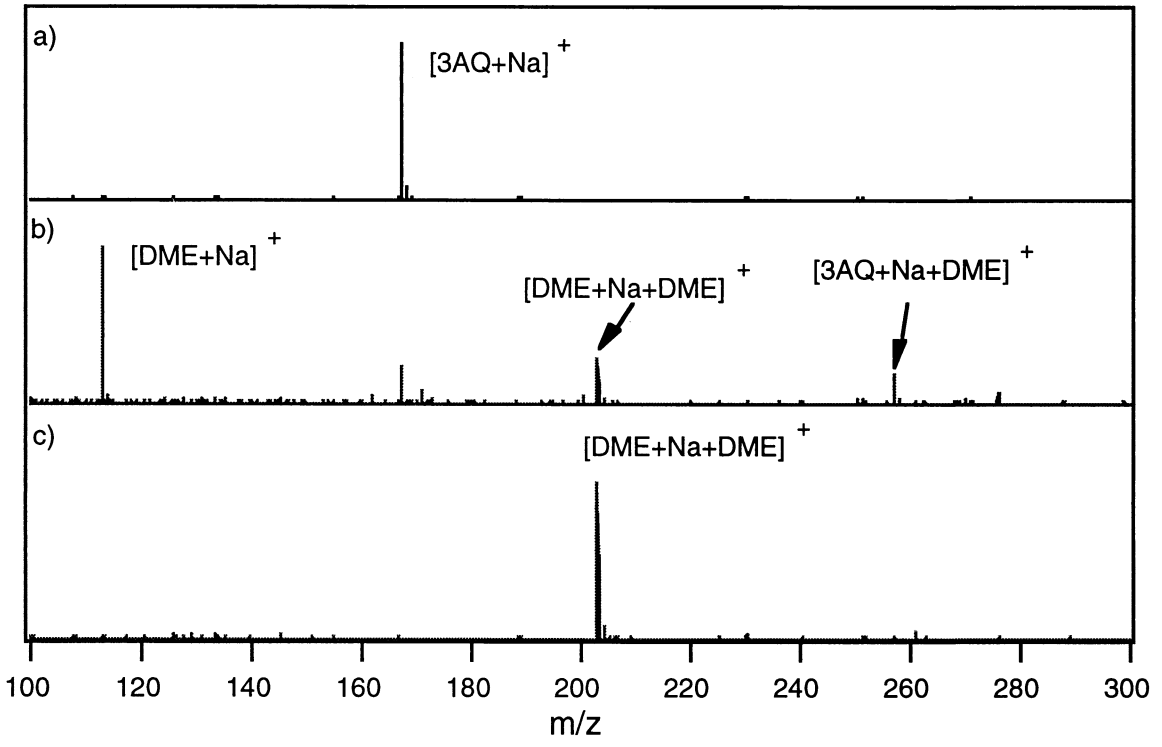

Fig. 1. Positive FT ICR mass spectra of sodium transfer reactions between sodiated 3-aminoquinoline and reference base DME after (a) 2 μs, (b) 10 s, and (c) 30 s reaction delays.

the cylindrical cell. Therefore, the vapor from sublimation of the solid sample filled the cell region and the vacuum system, giving a constant partial pressure of neutral matrix molecules [M]. This was verified by employing electron impact ionization (EI). The vapor pressure of most matrices studied in this work is quite low (in the range of 10^{-9} mbar [9]). Therefore, a direct determination of the matrix vapor pressure is difficult. Since the absolute values of neutral vapor pressure are not necessarily required in both the kinetic fits and the equilibrium methods, the ratio of the neutral matrix and reference base partial pressure was determined using electron impact ionization. Vapor of the reference base, which is a liquid at room temperature, was introduced through a leak valve. The typical electron energy used was 70–80 eV with 3–5 s ionization time.

The neutral molecules ionized by EI gave different ions, e.g. $[M]^{\cdot +}$, $[M + H]^+$, $[M]^{2+}$, etc. All these signals were summed and the ratio of two neutrals ([M]/[Re]) was calculated using these summed ion signals. EI provides relatively stable signal intensity. The uncertainty of the neutral ratio [M]/[Re] is then mainly due to the different ionization efficiencies. The ionization efficiencies of the matrices and Re were estimated from ion gauge sensitivity factors for similar compounds as given in the manual for the ion gauge. $S_{DME}/S_{N2} = 4 \pm 1$ was used for dimethoxyethane and $S_{matrix}/S_{N2} = 6 \pm 1$ for the matrices. The relative ionization sensitivity S_{DME}/S_{matrix} was used to correct the systematic error of the neutral ratio [M]/[Re].

The experiments were carried out at 298 K. The pressure of the neutral mixture in the ICR cell during the experiment was typically 3.0×10^{-8} mbar. The sodiated positive matrix ions were isolated with a SWIFT waveform, cooled down to room temperature, and then allowed to react with neutral reference base

molecules. Spectra were a summed over ten laser shots and taken after various reaction delays until the reaction approached equilibrium.

Matrices were purchased from Fluka (Buchs, Switzerland): 2,5-dihydroxy benzoic acid (DHB), para-nitroaniline (PNA), trans-3-methoxy-4-hydroxycinnamic acid (ferulic acid, FA), nicotinic acid (NA), trans-3,5-dimethoxy-4-hydroxycinnamic acid (sinapinic acid, SA), 3-hydroxypicolinic acid (3HPA), 4-hydroxy-α-cyanocinnamic acid (4HCCA), 3-aminoquinoline (3AQ), 6-aza-2-thiothymine (ATT), dithranol, and 2,4,6-trihydroxyacetophenone (THAP).

4. Quantum chemistry

All theoretical calculations were run using the Gaussian94 package [54]. Density functional theory (DFT) was used for frequency calculations. The geometry of the neutral and sodium-bound MALDI matrices were first optimized at the B3LYP/6-31+G * level. The vibrational frequencies, which are used for the calculation of the thermodynamic quantities, e.g. free energy, are also obtained at this level. The gas-phase sodium basicity of 2,5-dihydroxy benzoic acid was determined as the difference between the free energy value of the complex $[DHB + Na]^+$ and that of 2,5-dihydroxy benzoic acid and sodium ion.

5. Results and discussion

5.1. Direct determination of equilibrium constant

Fig. 1 illustrates typical spectra for the sodium ion transfer reaction between sodiated 3-aminoquinoline and the reference base dimethoxyethane at the beginning of reaction (Fig. 1(a)), after 10 (Fig. 1(b)) and 30 s (Fig. 1(c)). After 10 s reaction time the sodiated reference base $[DME + Na]^+$ is the dominant species although the sodium bound hetro dimer $[3AQ + Na + DME]^+$ and the homo dimer $[DME + Na + DME]^+$ are already clearly seen. After 30 s the sodium bounded homo dimer completely dominates the spectra.

The normalized intensity of the sodiated reference base does not remain constant as the reaction progresses, due to the competing reaction in which the homo dimer is produced (Fig. 2(a)). Thus, the sodium transfer reaction is taken to be complete once the sum of normalized intensities of sodiated DME ($[DME + Na]^+$) and the corresponding homo dimer ($[DME + Na + DME]^+$) remains constant: $d([DME + Na]^+ + [DME + Na + DME]^+)/dt = 0$ (see Fig. 2(b)). This quasiequilibrium is generally reached after 30s reaction time.

Grützmacher and coworkers have also observed homo dimer formation in proton transfer reactions. They found that in a gas-phase proton transfer the ratio of proton providing species and proton-accepting species remains constant after a certain reaction time [55]. This ratio was used for determination of the equilibrium constant. Since sodium ion transfer reactions are similar, it should be possible to use this method for determination of the equilibrium constant here.

However, if we consider Fig. 2(c), in which the ratio of sodiated 3-aminoquinoline and dimethoxyethane vs. reaction time is illustrated, we can see that the curve bends slightly upwards after a nearly flat region. This is inconsistent with the above-mentioned approach. The reason is found by inspecting Fig. 2(a). Fig. 2(a) shows that after 10 s reaction time the intensity of sodiated 3-aminoquinoline remains almost constant while the intensity of sodiated dimethoxyethane is still changing. In this case, the classic equilibrium method can only be used if we consider the constant region in Fig. 2(c) as a quasiequilibrium. Again, here, the formation of homo dimer is not treated properly.

5.2. Fit of the reaction kinetics

In order to fully account for the homo dimer formation, fitting of the kinetic data was employed, and the equilibrium constant can then be determined using equation 11. The time-dependent development of normalized ion intensities observed in the gas-phase sodium ion transfer reaction between sodiated 3-aminoquinoline and dimethoxyethane is illustrated in Fig. 2(a). The solid lines are kinetic fits. The two

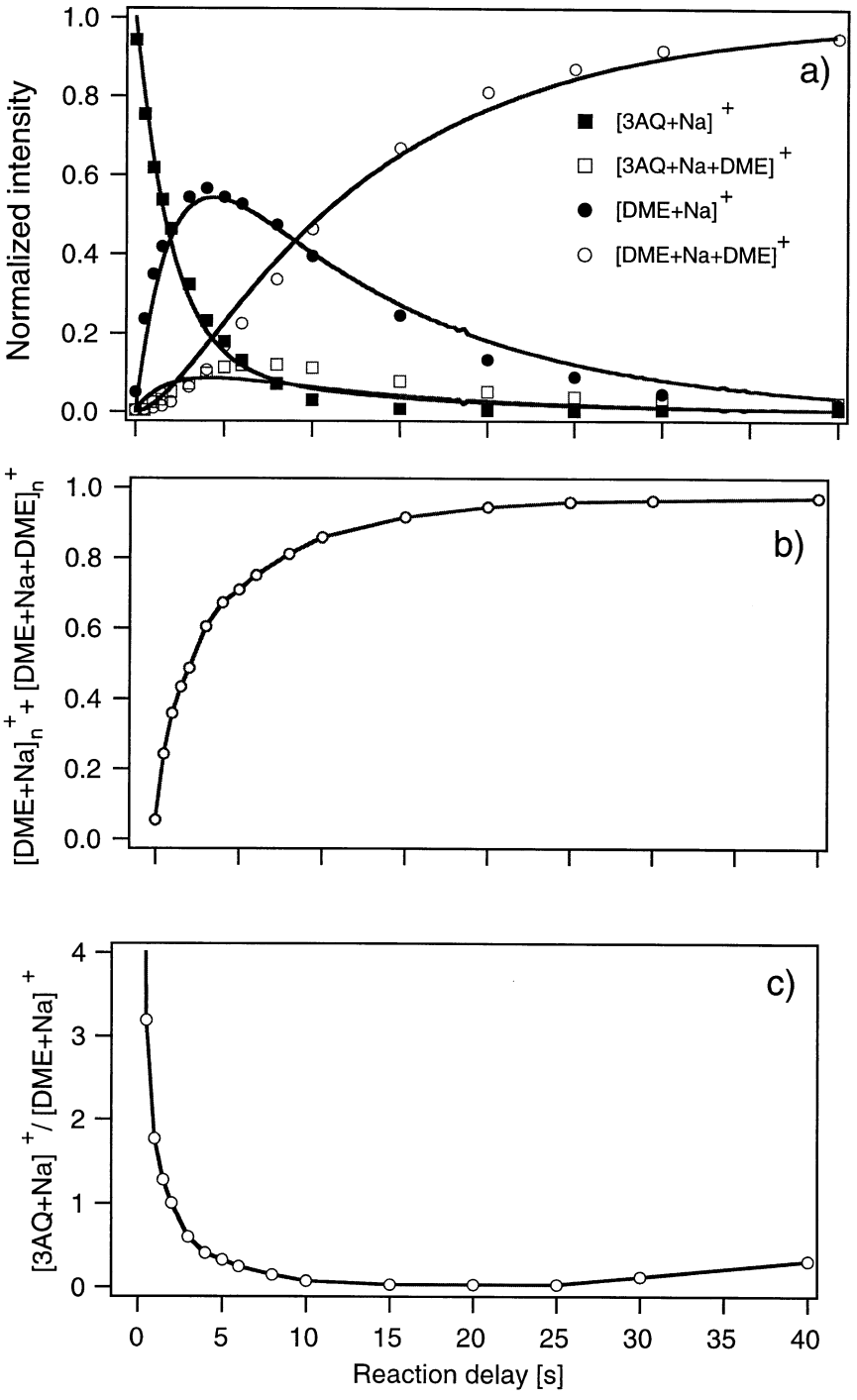

Fig. 2. Kinetic plot of gas-phase sodium ion transfer reaction between sodiated 3-aminoquinoline and dimethoxyethane; (a) plot of normalized intensities of observed ion species vs. reaction time. The solid lines are kinetic fit functions; (b) plot of the normalized intensities of $[DME + Na]^+ + [DME + Na + DME]^+$ vs. reaction time; (c) plot of ratio of intensities of sodiated 3-aminoquinoline and dimethoxyethane vs. reaction time.

models shown above were used to fit the data points. For most cases, model 2 gave a better fit quality. Nevertheless, the ΔG values determined by these two different models do not show significant differences. Thus, the fit was usually based on model 2, except in the case of dithranol.

Model 2 is not suitable for dithranol, because the sodiated dithranol transfers the sodium ions to dimethoxyethane without forming a sodium-bound hetro dimer ([dithranol + Na + DME]$^+$) with dimethoxyethane. This is a unique case among the matrices we studied. Fig. 3(a) illustrates the kinetics of the sodium ion transfer reaction between sodiated dithranol and dimethoxyethane. The solid lines are the kinetic fits (model 1). The sum of sodiated dimethoxyethane and the corresponding homo dimer remains constant after 30s reaction time (Fig. 3(b)).

The gas-phase sodium basicities of twelve MALDI matrices determined by two methods, together with literature values of their gas-phase proton affinities/basicities and the activation energies of the sodium transfer reaction are summarized in Table 1.

For para-nitroaniline there is no value from kinetic fitting, because the sodium ion transfer reaction between para-nitroaniline and dimethoxyethane becomes more complicated due to the formation of a homo dimer [PNA + Na + PNA]$^+$. This species was treated as a reagent, and the equilibrium method was used. The uncertainty of the ΔG-value is thus considerably larger.

The gas-phase sodium basicity of the reference base dimethoxyethane used in this work is GNaB(Re) = 154 kJ mol^{-1}, measured using high pressure mass spectrometry [35]. A value for the gas-phase sodium affinity of DME, $-\Delta H = 161 \pm 4$ kJ mol^{-1} has been obtained using the threshold CID method in a guided ion beam mass spectrometer [43]. Subtracting the estimated entropy change for sodium ion transfer puts the GNaB value into the same range as the one obtained in [35].

The estimated uncertainty of the sodium basicity from the fits is obtained by error propagation; including the error of the fit itself, the uncertainty of [M]/[Re] and the uncertainty in GNaB of the reference base. Error estimation in the kinetic fits requires estimated errors for individual data points. These were obtained from five repetitions at each reaction time. In the error analysis we have considered only two parameters, the equilibrium constant K_{eq} and the k_1-value, to limit the $\Delta\chi^2$ range which must be considered. The confidence level for this part of the error analysis was 68% ($1 - \sigma$) [48]. The value of [M]/[Re] is corrected by the relative ionization efficiencies, this only reduces the systematic error of the [M]/[Re] ratio. The estimated uncertainty of [M]/[Re] ($\pm 50\%$) was used in the kinetic fits, and the resulting error in K_{eq} and in ΔG is obtained. Finally, we also need the error of the reference base sodium basicity, which was assumed to be ± 0.3 kcal mol^{-1} from comparison with similar experimental uncertainties given in [35].

Error propagation was also employed in the error estimation for the equilibrium method. The ratio of ion intensities could be obtained from the mass spectra without a large error. The major contribution was the uncertainty in the ratio [M]/[Re], again taken as $\pm 50\%$. Including the error for the reference base we have obtained the estimated error of the sodium basicity (Table 1). Although this estimation includes all experimental factors, the influence of shifted equilibrium due to the sodium bound homo dimer has not been considered and therefore must be considered as a source of systematic error.

Comparing the values obtained by the two methods presented in Table 1, we can see that they differ by 3 kJ · mol^{-1} at most. Thus, assuming the existence of a quasi equilibrium is acceptable at the condition used in the experiments.

Recommended values are presented in Table 2. The GNaB-values from kinetic fitting are chosen for this approach, because this method gives more precise GNaB-values than the equilibrium method, and since it explicitly accounts for homo dimer formation. For para-nitroaniline there is no data from kinetic fitting, thus the value from the direct determination of the equilibrium constant was used in Table 2.

Table 2 shows that the measured gas-phase sodium basicities of all MALDI matrices studied are very similar. The values lie between 140–170 kJ mol^{-1}. This can be explained by the similarities in molecular

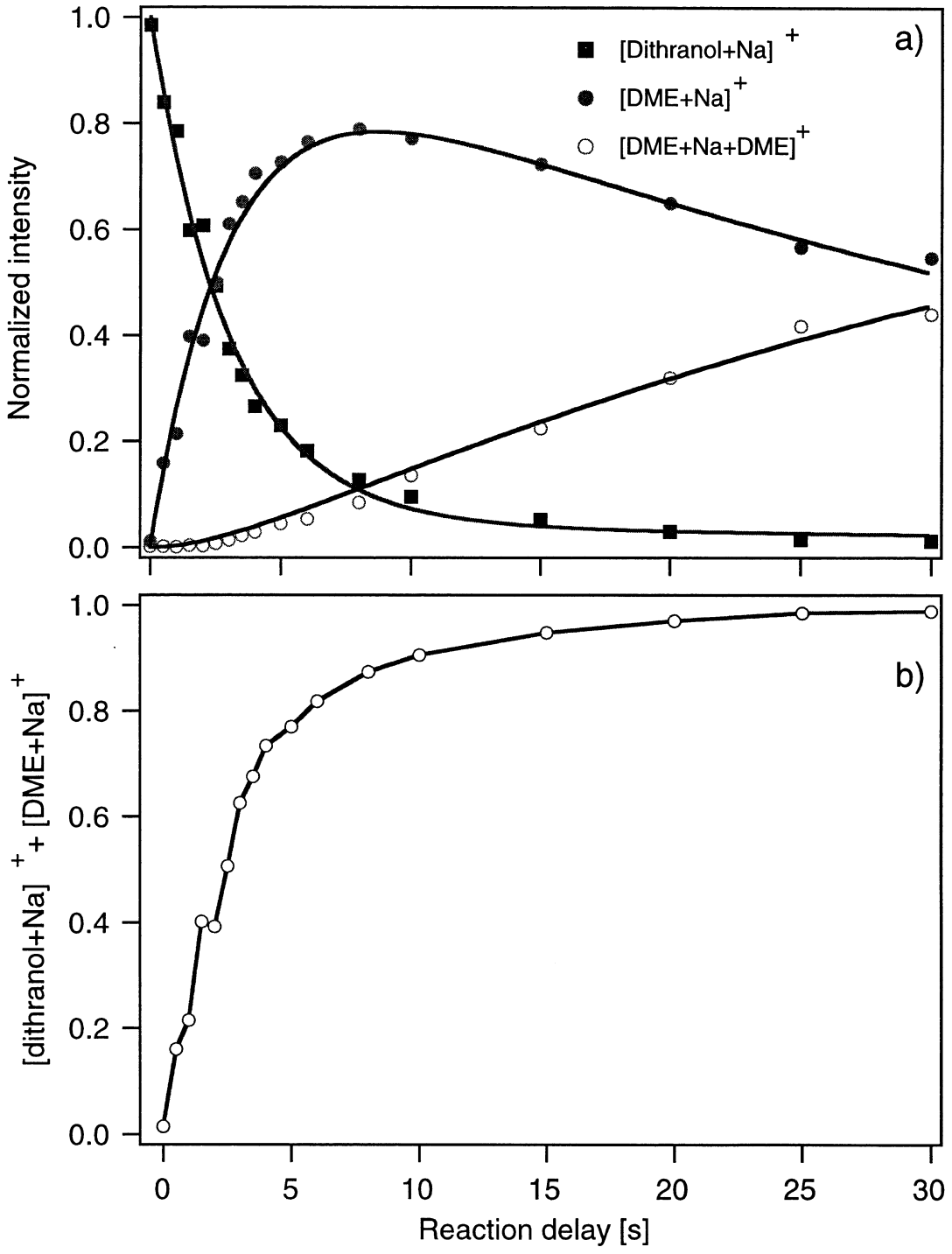

Fig. 3. Kinetic plot of gas-phase sodium ion transfer reaction between sodiated dithranol and dimethoxyethane; a) plot of normalized intensities of observed ion species vs. reaction time. The solid lines are kinetic fit functions; b) plot of the normalized intensities of $[DME + Na]^+ + [DME + Na + DME]^+$ vs. reaction time.

Table 1
Gas-phase sodium basicities (GNaB), activation energy (Ga) and gas-phase proton affinity or basicity of common MALDI matrices; **Kin.**: equilibrium constants were determined by fitting of complete reaction kinetics; **Equ.**: direct determination of equilibrium constants

Matrices	GNaB (kJ mol^{-1})		Activation energy Ga ± 1 (kJ mol^{-1})	GB (kJ mol^{-1})
	Kin.	Equ.		
NA	166 ± 1	167 ± 5	9	907 [30]
4HCCA	165 ± 3	166 ± 3	6	841 [30]
				900.5 ± 8.5 [8]
3HPA	163 ± 3	161 ± 4	8	896 [30]
ATT	161 ± 3	162 ± 1	7	–
FA	160 ± 2	163 ± 6	6	879 [30]
SA	159 ± 2	162 ± 5	7	887 [30]
DHB	158 ± 3	159 ± 2	7	854 ± 14 [8]
				848 [28]
PNA	–	157 ± 2	–	866 [29]
THAP	154 ± 2	155 ± 2	5	878 [28]
Dithranol	150.5 ± 0.5	149 ± 2	6	875 ± 8 [7]
3AQ	144.3 ± 2	144 ± 1	6	–

structure of the matrices: most of them have an aldehyde or carboxyl functional group. The oxygens on these functional groups are responsible for the complexation of the sodium ion. Besides oxygen, nitrogen atoms can also play a role in the complexation of the sodium ion, e.g. in the case of 3-aminoquinoline.

The relative GNaB-values anchored to that of 3-aminoquinoline are also given in Table 2. There are two reasons for this: first, for MALDI users, it is more relevant to know the order of the gas-phase sodium basicities of the matrices than the absolute values. Second, the error bars of the relative values are much smaller than that of the absolute values. This is because systematic errors, such as uncertainties of the reference base GNaB cancel. Thus, the order of the sodium basicities becomes more clear and precise, and was found to be: NA > 4HCCA > 3HPA > ATT > FA > SA > DHB > PNA > THAP > Dithranol > 3AQ.

Table 2
The recommended gas-phase sodium basicities (data are selected from K = fitting of reaction kinetics, E = equilibrium method) and the relative values anchored to the value of THAP

Matrices	GNaB (kJ mol^{-1})	
	Recommended values	Relative values (±1 kJ mol^{-1})
NA	166 ± 1^{K}	22
Cyano	165 ± 3^{K}	21
3HPA	163 ± 3^{K}	18
ATT	161 ± 3^{K}	16
FA	160 ± 2^{K}	16
SA	159 ± 2^{K}	15
DHB	158 ± 3^{K}	13
PNA	157 ± 2^{E}	13
THAP	154 ± 2^{K}	10
dithranol	150.5 ± 0.5^{K}	6
3AQ	144 ± 2^{K}	0

5.2. Computations of GNaB

Density functional calculations using the B3LYP hybrid function are in progress to estimate GNaB values theoretically. A preliminary result of the calculations is given here for the cationization of 2,5-dihydroxy benzoic acid. The theoretically determined sodium basicity of 2,5-dihydroxybenzoic acid is 160 kJ mol^{-1}, in very good agreement with the experimental result, 158 kJ mol^{-1}; the difference is only 2%. This suggests that the computational method can be applied in the future to obtain thermodynamic values such as gas-phase sodium basicities, in cases where experimental values are not available. From the calculations, we also obtain the conformation of the sodium complex, which is not available from our experimental data. Fig. 4 and 5 shows two of the most stable structures of DHB-Na^+-complex. Structure **b** is less stable than structure **a**, they differ by 4 kJ·mol^{-1} in total energy. The sodium ion in the DHB-Na^+-complex binds to the oxygen atoms of the carboxyl and hydroxyl functional group, and sits in the molecular plane. The implications of this will be discussed below.

Ohanessian and coworkers have compiled sodium affinity data for various organic compounds and molecules of biological interest [37]. The sodium affinities of most amino acids cited are greater than 150 kJ mol^{-1} and values for dipeptides usually lie above 160 kJ mol^{-1}. The gas-phase sodium affinities of nucleobases were reported to lie between 164–190

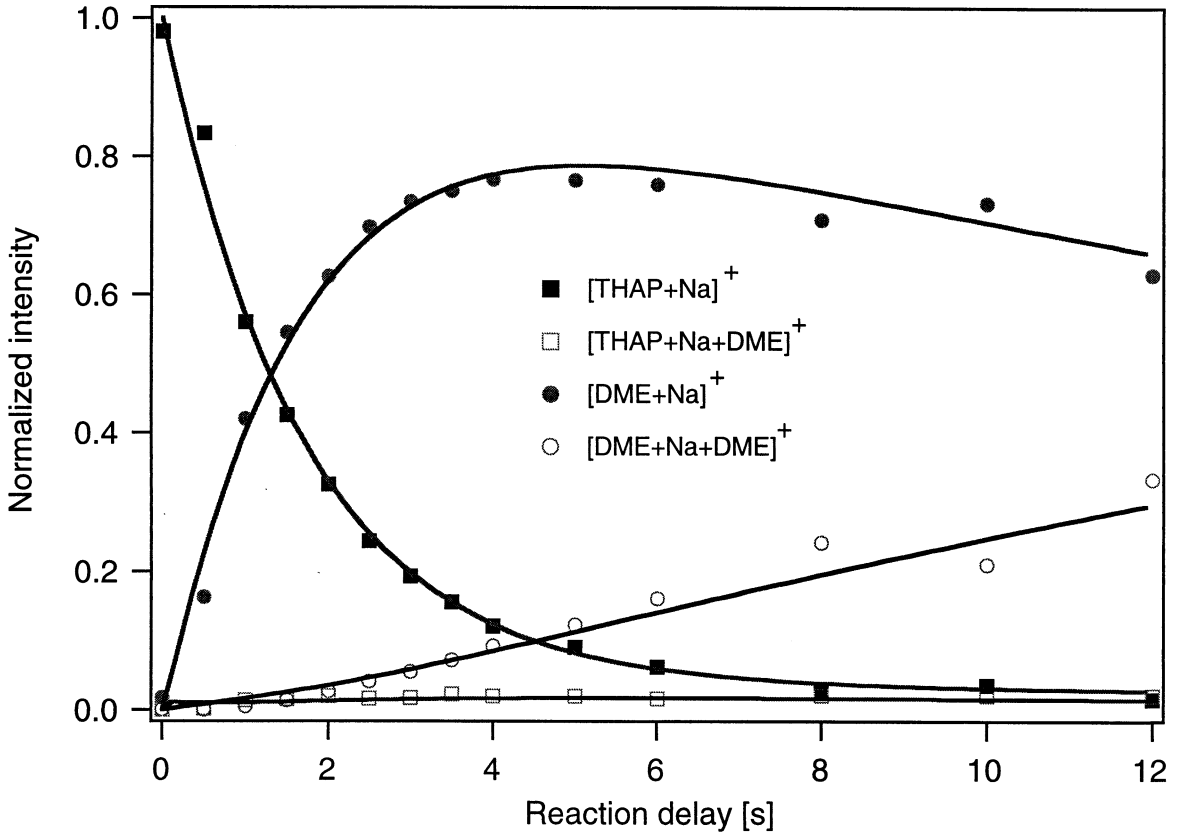

Fig. 4. Kinetic plot of gas-phase sodium ion transfer reaction between sodiated 2,4,6-trihydroxyacetophenone and dimethoxyethane. The solid lines are kinetic fit functions.

kJ mol^{-1} [32]. Carbohydrates also have relatively high sodium affinities (≥160 kJ mol^{-1}). Among all matrices studied dithranol has one of the lowest gas-phase sodium basicities, 150 kJ mol^{-1}. If we consider a gas-phase sodium transfer reaction in the MALDI plume,

$$[Dithranol + Na]^+ + Analyte \xrightarrow{\Delta G} Dithranol + [Analyte + Na]^+$$

$$\Delta G = -15 \sim -40 \text{ kJ mol}^{-1} \quad (14)$$

it is clear that the reaction is exoergic for all of the analytes listed above.

This may explain why dithranol is often used as a matrix when cationization is desired, for example, for the analysis of polymers that are not easily protonated [23]. 3-aminoquinoline also has relatively low sodium basicity. Although this matrix has not been used often as a matrix for polymers [23], our result suggests that 3-aminoquinoline may be a useful matrix for polymer analysis.

The proton affinities (ΔH) of the matrices given in Table 1 are obviously much higher than the sodium basicities. The driving force for formation of sodium complexes is expected to be largely electrostatic interaction between the sodium ion as an electron acceptor, and O or N atoms of the matrix molecules as electron donors. The situation for protonation should be similar. We would therefore expect a correlation between the sodium basicities and the proton affinities/basicities. However, as it is shown in Table 2, no

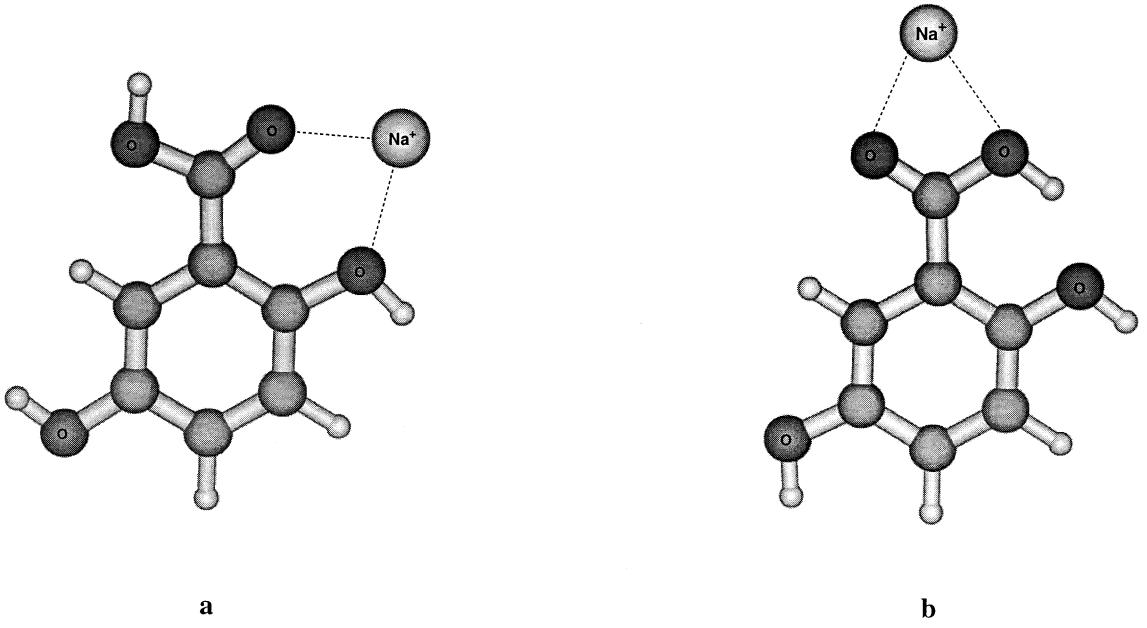

Fig. 5. Conformations of two $[DHB+Na]^+$ complexes obtained from quantum chemical computations.

clear correlation between the proton affinities and the sodium basicities is observed. This indicates that electrostatic interactions are not the only factor that determines proton/cation binding. For the case of a matrix with a carboxyl group, binding of sodium to both oxygens significantly increases the binding energy of the complex compared to complexation by only a single oxygen atom. This does not occur in the case of protonation, since the proton is too small to be bound to both oxygens. In addition to the electrostatic interaction, structure is thus another important factor determining the gas-phase sodium basicity/affinity, and probably the explanation for the lack of a correlation between proton and sodium basicities/affinities.

In contrast to sodium ion transfer, proton transfer reactions that were investigated on the same instrument and under the same conditions required less than 20s to reach equilibrium [9]. This indicates that the activation energy for sodium ion transfer in the gas-phase must be higher than the activation energy for proton transfer. As we discussed in introduction, steric hindrance and charge delocalization are the most important reasons for the difference between sodium ion transfer and proton transfer.

The activation energies G_a determined by Eq. 12 are also presented in Table 1. The reaction rate constants employed in Eq. 12 were the k_1-values obtained from the kinetic fit. The dissociation reaction of the hetro dimer is obviously very fast, such that we do not see much hetro dimer. This also indicates that the first step of the sodium transfer reaction, i.e. the formation of the hetro dimer, is the rate-limiting step. The activation energies given in Table 1 are all under 10 kJ mol^{-1}, which is much smaller than the thermal energy of molecules in a MALDI plume (typical plume temperatures are about 500 K). This energy barrier for sodium transfer in the MALDI plume is therefore not difficult to overcome. At least for sodium, this argues against kinetic control in MALDI ion formation by cation attachment [2].

6. Conclusions

The gas-phase sodium basicities (GNaB) of eleven MALDI matrices were determined in this work using the equilibrium method and by a complete fit of the reaction kinetics. The activation energies for gas-

phase sodium ion transfer could also be estimated using a calculated ion-neutral collision rate constant in the ICR cell. Gas-phase sodium basicities for all MALDI matrices studied were found to lie around 150 kJ mol^{-1} and were much lower than the corresponding proton basicities/affinities of the matrices. The best matrix for cationization in polymer analysis, dithranol, has one of the lowest sodium basicities among the matrices investigated. This might be the explanation for the intense cationized signals in MALDI MS spectra if dithranol is used as the matrix. Finally, arguments in support of thermodynamic control in MALDI ion formation by sodium attachment were presented.

Acknowledgement

This work has been funded by the Swiss Federal Institute of Technology. We thank Dr. Tea-Kyu Ha and Dr. Harold Baumann for their suggestions in quantum chemical computing.

References

[1] R. Zenobi, R. Knochenmuss, Mass Spectrom. Rev. 17 (1998) 337.
[2] R. Knochenmuss, A. Stortelder, K. Breuker, R. Zenobi, J. Mass Spectrom. 35 (2000) 1237.
[3] M.G. Kinsel, L.M.P. Schaffter, G.R. Kinsel, J. Am. Chem. Soc. 119 (1997) 2534.
[4] P.-C. Liao, J. Allison, J. Mass Spectrom. 30 (1995) 408.
[5] H. Ehring, M. Karas, F. Hillenkamp, Org. Mass Spectrom. 27 (1992) 472.
[6] C.M. Land, G.R. Kinsel, Abstr. Pap. Am. Chem. Soc. 215 (1998) U75.
[7] R.D. Burton, C.H. Watson, J.R. Eyler, G.L. Lang, D.H. Powell, M.Y. Avery, Rapid Commun. Mass Spectrom. 11 (1997) 443.
[8] R.J.J.M. Steenvoorden, K. Breuker, R. Zenobi, Eur. Mass Spectrom. 3 (1997) 339.
[9] K. Breuker R. Knochenmuss, R. Zenobi, Int. J. Mass Spectrom. Ion Proc. 184 (1999) 25.
[10] K. Breuker, R. Knochenmuss, R. Zenobi, J. Am. Soc. Mass Spectrom. 10 (1999) 1111.
[11] R. Knochenmuss, F. Dubois, M.J. Dale, R. Zenobi, Rapid Commun. Mass Spectrom. 10 (1996) 871.
[12] R. Knochenmuss, V. Karbach, U. Wiesli, K. Breuker, R. Zenobi, Rapid Commun. Mass Spectrom. 12 (1998) 529.
[13] C.K.L. Wong, T.-W.D. Chan, Rapid Commun. Mass Spectrom. 11 (1997) 517.
[14] H. Rashidezadeh, Y. Wang, B. Guo, Rapid Commun. Mass Spectrom. 14 (2000) 439.
[15] H. Rashidezadeh, Y. Wang, B. Guo, Am. Soc. Mass. Spectrom. (1999).
[16] H. Cheng, P.A.C. Clark, S.D. Hanton, P. Kung, J. Phys. Chem. A 104 (2000) 2647.
[17] M.J. Deery, K.R. Jennings, C.B. Jasieczek, D.M. Haddleton, A.T. Jackson, H.T. Yates, J.H. Scrivens, Rapid Commun. Mass Spectrom. 11 (1997) 57.
[18] T. Fujii, Mass Spectrom. Rev. 19 (2000) 111.
[19] A.-M. Hoberg, D.M. Haddleton, P.J. Derrick, Eur. Mass Spectrom. 3 (1997) 471.
[20] R. Knochenmuss, E. Lehmann, R. Zenobi, Eur. Mass Spectrom. 4 (1998) 421.
[21] H. Rashidezadeh, B. Guo, J. Am. Soc. Mass Spectrom. 9 (1998) 724.
[22] H. Rashidezadeh, K. Hung, B. Guo, Eur. Mass Spectrom. 4 (1998) 429.
[23] M.W.F. Nielen, Mass Spectrom. Rev. 18 (1999) 309.
[24] M.E. Belov, C.P. Myatt, P.J. Derrick, Chem. Phys. Lett. 284 (1998) 412.
[25] F. Hillenkamp, M. Karas, R.C. Beavis, B.T. Chait, Anal. Chem. 63 (1991) 1193a.
[26] M. Karas, U. Bahr, K. Strupat, F. Hillenkamp, A. Tsarbopoulos, B.N. Pramanik, Anal. Chem. 67 (1995) 675.
[27] S. North, G. Okafo, H. Birrell, N. Haskins, P. Camilleri, Rapid Commun. Mass Spectrom. 11 (1997) 1635.
[28] C.M. Nelson, L. Zhu, W. Tang, L.M. Smith, K. Crellin, J. Berry, J.L. Beauchamp, SPIE 2680 (1996) 247.
[29] E.P. Hunter, S.G. Lias, J. Phys. Chem. Ref. Data 27 (1998) 413.
[30] T.J.D. Jørgensen, G. Bojesen, H. Rahbek-Nielsen, Eur. Mass Spectrom. 4 (1998) 39.
[31] B.A. Cerda, S. Hoyau, G. Ohanessian, C. Wesdemiotis, J. Am. Chem. Soc. 120 (1998) 2437.
[32] J.S. Klassen, S.G. Anderson, A.T. Blades, P. Kebarle, J. Phys. Chem. 100 (1996) 14218.
[33] R. Amunugama, M.T. Rodgers, Int. J. Mass Spectrom. Ion Processes 195/196 (2000) 439.
[34] A.M.P. Borrajo, J.-F Gal, P.-C. Maria, M. Decouzon, D.C. Ripley, E. Buncel, G.R.J. Thatcher, J. Org. Chem. 62 (1997) 9203.
[35] B. Guo, B.J. Conklin, A.W. Castleman Jr., J. Am. Chem. Soc. 111 (1989) 6506.
[36] B. Guo, J.W. Purnell, A.W. Castleman Jr., Chem. Phys. Lett 168 (1990) 155.
[37] S. Hoyau, K. Norrman, T.B. McMahon, G. Ohanessian, J. Am. Chem. Soc. 121 (1999) 8864.
[38] A.W. Castleman Jr., P.M. Holland, D.M. Lindsay, K.I. Peterson, J. Am. Chem. Soc. (1978) 6039.
[39] B.A. Cerda, C. Wesdemiotis, J. Am. Chem. Soc. (1996) 11884.
[40] R.G. Cooks, J.S. Patrick, T. Kotiaho, S.A. McLuckey, Mass Spectrom. Rev. 13 (1994) 287.
[41] G. Bojesen, T. Breindahl, U.N. Andersen, Org. Mass Spectrom. 28 (1993) 1448.
[42] W.Y. Feng, S. Gronert, C.B. Lebrilla, J. Am. Chem. Soc. 121 (1999) 1365.

[43] M.B. More, D. RaY, P.B. Armentrout, J. Phys. Chem. A 101 (1997) 831.
[44] N.F. Dalleska, B.L. Tjelta, P.B. Armentrout, J. Phys. Chem. 98 (1994) 4191.
[45] M.T. Rodgers, P.B. Armentrout, Int. J. Mass Spectrom. 185 (1999) 359.
[46] I. Dzidic, P. Kebarle, J. Phys. Chem. 74 (1970) 1466.
[47] M.B. More, D. Ray, P.B. Armentrout, J. Am. Chem. Soc. 121 (1999) 417.
[48] W.H. Press, B.P. Flannery, S.A. Teukolsky, W.T. Vetterling, Numerical Recipes- The Art of Scientific Computing, Cambridge University Press, Cambridge, 1988.
[49] J.A. Dodd, S. Baer, C.R. Moylan, J.I. Brauman, J. Am. Chem. Soc. 113 (1991) 5942.
[50] N. Agmon, Int. J. Chem. Kin. 13 (1981) 333.
[51] J.I. Steinfeld, J.S. Francisco, W.L. Hase, Chemical Kinetics and Dynamics, Prentice Hall, Englewood Cliffs, NJ, 1989.
[52] S.M. Ponomarenko, S.P. Mushtakova, A.G. Demakhin, B.L. Faifel, D.G. Kal'manovich, Russ. J. Gen. Chem.65 (1995) 190.
[53] M. Dale, R. Knochenmuss, R. Zenobi, Rapid. Commun. Mass Spectrom. 11 (1997) 136.
[54] M.J. Frisch, G.W. Trucks, H.B. Schlegel, P.M.W. Gill, B.G. Johnson, M.A. RobB, J.R. Cheeseman, T. Keith, G.A. Petersson, J.A. Montgomery, K. Raghavachari, M.A. Al-Laham, V.G. Zakrzewski, J.V. Ortiz, J.B. Foresman, J. Cioslowski, B.B. Stefanov, A. Nanayakkara, M. Challacombe, C.Y. Peng, P.Y. Ayala, W. Chen, M.W. Wong, J.L. Andres, E.S. Replogle, R. Gomperts, R.L. Martin, D.J. Fox, J.S. Binkley, D.J. Defrees, J. Baker, J.P. Stewart, M. Head-Gordon, C. Gonzalez, J.A. Pople, Revesion C. 3, Gaussian, Inc., Pittsburgh, 1995.
[55] M. Witt, H.-F. Grützmacher, Int. J. Mass Spectrom. 164 (1997) 93.